Scientific Reports

https://doi.org/10.1038/s41598-026-67846-7

Article in Press

Linking molecular antioxidant activity to polyurethane foam stability - the case of *Abies marocana* essential oil

Received: 3 February 2026

Accepted: 18 August 2026

Published online: 21 August 2026

Cite this article as: El Bakkali M., Thbayh D.K., Mentes D. *et al.* Linking molecular antioxidant activity to polyurethane foam stability - the case of *Abies marocana* essential oil. *Sci Rep* (2026). https://doi.org/10.1038/s41598-026-67846-7

Mohamed El Bakkali, Dalal K. Thbayh, Dóra Mentes, László Farkas, Dávid Salamon, Anikó Csábrádiné Jordán, Béla Viskolcz, Amin Bouchfara, Badredine Souhail, Mounir Nechar, Rehana Bano & Béla Fiser

Linking Molecular Antioxidant Activity to Polyurethane Foam Stability - The Case of *Abies marocana* Essential Oil

Mohamed El Bakkali[1], Dalal K. Thbayh[2,3], Dóra Mentes[3,4], László Farkas[3],

Dávid Salamon[3,4], Anikó Csábrádiné Jordán[3,4], Béla Viskolcz[3,4], Amin Bouchfara[1],

Badredine Souhail[1], Mounir Nechar[1], Rehana Bano[3], Béla Fiser[3,4,5,*]

[1] Laboratory of Water, studies and Environmental Analysis, Faculty of Sciences, Tétouan, Abdelmalek Essaâdi University, Morocco

[2] Polymer Research Center, University of Basrah, Basrah, Iraq

[3] Higher Education and Industrial Cooperation Centre, University of Miskolc, 3515 Miskolc-Egyetemváros, Hungary

[4] Institute of Chemistry, University of Miskolc, 3515 Miskolc-Egyetemváros, Hungary

[5] Department of Physical Chemistry, Faculty of Chemistry, University of Lodz, 90-236 Lodz, Poland

* Corresponding author: Béla Fiser, bela.fiser@uni-miskolc.hu

Abstract

In this work, compounds from *Abies marocana* essential oil (AMEO) were studied for their antioxidant potential using density functional theory (DFT) calculations at the M06-2X/6-311+G(d,p) level of theory. The antioxidant activity was evaluated through three mechanistic pathways: hydrogen atom transfer (HAT), single electron transfer–proton transfer (SET-PT), and sequential proton loss–electron transfer (SPLET). The corresponding thermodynamic descriptors, including bond dissociation enthalpy (BDE), ionization potential (IP), proton dissociation enthalpy (PDE), proton affinity (PA), and electron transfer enthalpy (ETE), were calculated in the gas phase, while the HAT mechanism was additionally investigated in water and ethylene glycol to assess solvent effects. Additionally, frontier molecular orbital (FMO) analysis revealed that α-pinene possesses the smallest HOMO-LUMO energy gap (E_g), followed by limonene, further supporting the higher chemical reactivity and radical scavenging potential of these compounds. The influence of the studied essential oil as a natural antioxidant additive at varying concentrations on the thermal degradation (ageing) of flexible polyurethane foams was also assessed. Compression tests before and after dry heat ageing indicated that AMEO-modified foams showed improved compression-force retention compared with the reference sample. Higher AMEO concentrations increased the absolute compression force before and after ageing, while the calculated percentage compression-force loss was generally lower than that of the reference sample, indicating improved ageing resistance. Fourier transform infrared spectroscopy (FTIR) analysis suggested that AMEO does not form strong chemical interactions with the polyurethane matrix, supporting a physical radical scavenging mechanism. These

results suggest that AMEO can serve as a multifunctional additive in polyurethane foams, providing both antioxidant activity and mechanical property tuning.

Keywords: *Abies marocana;* flexible polyurethane foam; DFT; ageing; mechanical tests.

1. Introduction:

Natural compounds that can be obtained from various medicinal and aromatic plants have gained recognition as alternative treatments and raw materials for various applications [1,2]. These are widely used in medicine, modern drug research, cosmetics, functional foods, construction, packaging material, and as environmentally friendly agents in nanotechnology to synthesize metallic nanoparticles with biomedical and industrial applications [1]. Medicinal and aromatic plants are important sources of bioactive compounds, especially essential oils (EOs), which are volatile liquids extracted from different parts of aromatic plants such as barks, seeds, flowers, peels, roots, leaves, wood, fruits, and whole plants and are named according to their botanical origin [3,4]. EOs can be extracted using various methods, including hydro-distillation, steam distillation, hydro-diffusion, and solvent extraction [5]. These volatile secondary metabolites are composed mainly of terpenes and phenolics, and they exhibit a wide range of biological activities, including antibacterial, antifungal, and particularly antioxidant properties [6].

Plant-derived EOs have found applications in various food industries [7]. In recent years, they have gained recognition for their antioxidant properties, which make them effective agents for food preservation [8]. However, designing suitable packaging for specific foods can be challenging, as certain compounds from packaging materials may migrate into the food, posing potential toxicity risks [9]. When applied in food systems, EOs can serve antimicrobial, antioxidant, or flavoring functions [10]. Among these, their primary role is to inhibit or eliminate microbial growth and reduce lipid oxidation [11]. EOs may be incorporated directly into food, enclosed within separate containers, or integrated into packaging materials to enhance food safety and shelf life [12]. Although various antioxidants such as trolox and α-tocopherol have been extensively studied in polymeric systems, their mechanisms of action and suitability in food packaging formulations remain subjects of ongoing research [13,14]. In this context, natural antioxidants like EOs represent a promising alternative for incorporation into polymer-based packaging, offering both functionality and safety, while aligning with the growing demand for sustainable and bio-based materials [15]. Among these, *Abies marocana*, an endemic fir species from the Rif Mountains of northern Morocco [16], produces an essential oil. In this study, AMEO was found to be rich in monoterpenes, suggesting its potential as a natural antioxidant stabilizer for polymeric materials.

Polymeric materials, such as foams, can be rigid, flexible, or elastomeric and are produced from a wide variety of polymers, including [17] polyurethane (PU), polystyrene (PS), polyisocyanurate (PIR),

polyethylene (PE), polypropylene (PP), poly(ethylene-vinyl acetate) (EVA), nitrile rubber (NBR), poly(vinyl chloride) (PVC), and other polyolefins. Among these, global foam production is dominated by PU foams (PUFs), followed by PS and PVC foams [18,19].

Polyurethanes, in particular are a major class of polymers with broad industrial applications [20]. They are highly versatile and are formed through the reaction of polyols and isocyanates [21], and their performance is largely determined by two key parameters: density and rigidity [22]. Owing to these properties, PUs are widely used in the manufacture of plastics, cushions, foams, rubber goods, synthetic leathers, and fibers. Additional applications include the furniture, construction, and footwear industries, as well as various medicinal and agricultural fields [23]. Flexible polyurethane foams (FPUFs), on the other hand, were selected in this study as model systems. FPUFs are complex porous materials commonly used in comfort-related applications, including automotive seating and cushioning, due to their lightweight structure, durability, and excellent mechanical properties [23], but potentially applicable as food packaging materials especially protecting fruit and vegetables. For example, a bio-based polyurethane foam derived from soybean polyol and zein exhibited excellent cushioning and ethylene-absorbing properties, maintaining the appearance of tomatoes even after repeated drop tests from a height of 1.5 m [24].

Fruits and vegetables are often transported over long distances, which exposes them to mechanical stresses that can cause bruising or other damage [25,26]. To minimize such damage, packaging materials need to be soft and cushioning, with specific mechanical properties tailored to absorb shocks [27]. Flexible or elastomeric polymer foams, such as polyurethane foams, are ideal candidates for several applications, as they provide lightweight, durable, and resilient cushioning [28-30]. In this context, incorporating natural antioxidants like AMEO into FPUFs could further enhance their performance and stability, suggesting that AMEO-modified foams may be a promising solution for protecting fruits and vegetables during transport.

The antioxidant activity of phenolic compounds can proceed through several distinct mechanisms, among which hydrogen atom transfer (HAT), single electron transfer-proton transfer (SET-PT), and sequential proton loss-electron transfer (SPLET) are the most widely studied and relevant. In the hydrogen atom transfer (HAT) mechanism, the bond dissociation enthalpy (BDE) serves as a key descriptor of antioxidant potential [31]. Lower BDE values correspond to easier hydrogen donation, which enhances radical scavenging ability [32]. In the SET-PT mechanism, the antioxidant first donates an electron to the radical, forming a radical cation, and then transfers a proton. This mechanism is characterized by two thermodynamic parameters: the ionization potential (IP), which describes the ease of electron donation, and the proton dissociation enthalpy (PDE), which reflects the subsequent proton transfer step. Lower IP values indicate a greater propensity for electron donation and, thus, higher antioxidant activity through this pathway. In the SPLET mechanism, the antioxidant first loses a proton to form a phenoloxide anion, which

in turn donates an electron to the free radical. This pathway is described by the proton affinity (PA), which reflects the ease of the initial proton removal, and the electron transfer enthalpy (ETE), characterizing the subsequent electron donation step. SPLET is considered particularly relevant in polar and protonic environments [33]. In addition to thermodynamic descriptors, frontier molecular orbital (FMO) analysis, including HOMO and LUMO energies and the HOMO-LUMO energy gap (E_g), provides complementary information on the chemical reactivity and electron donation ability of antioxidant molecules [34,35]. Computational chemistry approaches provide a powerful tool for predicting these parameters and comparing antioxidant performance at the molecular level [36].

While several studies have investigated synthetic antioxidants in polymer systems, limited attention has been given to EOs derived compounds, and no systematic computational evaluation of AMEO compounds as potential natural antioxidant additives in polyurethane foams has been reported.

Based on this context, the present study investigates seven major constituents of AMEO (–)-limonene, (+)-limonene, (+)-*α*-pinene, (–)-*α*-pinene, (+)-*β*-pinene, (–)-*β*-pinene and camphene using a DFT approach at the M06-2X/6-311+G(d,p) level of theory. The antioxidant potential of these compounds was evaluated through three complementary mechanistic pathways: HAT, SET-PT, and SPLET, characterized by the thermodynamic descriptors BDE, IP, PDE, PA, and ETE, respectively. The thermodynamic parameters were evaluated in both the gas and solvent phases. In addition, FMO analysis was performed to further investigate the electronic properties and reactivity of the compounds studied. Enantiomers are expected to show identical values, as these parameters depend only on the bond type and local electronic environment, not on overall stereochemistry [37]. Furthermore, the potential application of AMEO as antioxidant additives in polyurethane formulations has been explored. In addition, the possible future use of the material in food-packaging applications is briefly discussed, although its suitability remains to be established through migration, toxicity, additive retention, and application-specific performance studies.

2. Materials and methods

2.1. Computational Details

2.1.1. Methods

Calculations were performed using Gaussian 16 program [38] at the M06-2X/6-311+G(d,p) level of theory in the gas, water, and ethylene glycol phases. The solvent effects of water and ethylene glycol were described using the solvation model based on density (SMD). The M06-2X functional has been effectively utilized before to study thermochemistry, kinetics, and non-covalent interactions, particularly in free radical processes [39]. The M06-2X functional was selected because a dedicated benchmarking study highlighted it as the most reliable method for BDE calculations, outperforming both B3LYP and M06. Specifically, B3LYP underestimated BDE values by more than 40 kJ/mol and M06 by more than 20 kJ/mol, while M06-

2X reproduced experimental values with deviations of only 6-7.5 kJ/mol [40-42]. However, since only terpenes were identified in this essential oil, the bond dissociation enthalpy (BDE), ionization potential (IP), proton dissociation enthalpy (PDE), proton affinity (PA), and electron transfer enthalpy (ETE) calculations were restricted to C–H bonds. Structures of AMEO compounds and their corresponding species (radicals, radical cations, and anions) were optimized. Each unique C–H position was determined, and the corresponding species were generated through hydrogen atom abstraction, electron removal, or proton dissociation, depending on the investigated mechanism [41].

2.1.2. Antioxidant Mechanism

The antioxidant mechanisms of AMEO compounds were systematically studied and comparatively analyzed according to three main pathways: HAT, SET-PT, and SPLET. The calculations were performed in the gas phase, with the exception of the HAT mechanism, which was also evaluated in ethylene glycol and water to better account for solvent effects. The main thermodynamic parameters associated with each mechanism, BDE, (**Equation 1**), IP, (**Equation 2**), PDE, (**Equation 3**), PA, (**Equation 4**), and ETE, (**Equation 5**), were determined and used as descriptors for evaluating and comparing the antioxidant potential of the studied molecules. This comprehensive approach provides a better understanding of the predominant reaction pathways and the relative efficacy of AMEO compounds as antioxidants under different conditions.

HAT mechanism:

$$BDE = H(A^{\bullet}) + H(H^{\bullet}) - H(A) \qquad \textbf{Equation 1}$$

SET-PT mechanism:

$$IP = H(A^{\bullet +}) + H(e^{-}) - H(A) \qquad \textbf{Equation 2}$$

$$PDE = H(A^{\bullet}) + H(H^{+}) - H(A^{\bullet +}) \qquad \textbf{Equation 3}$$

SPLET mechanism:

$$PA = H(A^{-}) + H(H^{+}) - H(A) \qquad \textbf{Equation 4}$$

$$ETE = H(A^{\bullet}) + H(e^{-}) - H(A^{-}) \qquad \textbf{Equation 5}$$

The enthalpies of the electron ($H(e^-)$) and proton ($H(H^+)$) in the gas phase are 3.1351 kJ/mol and 6.1398 kJ/mol, respectively [41,43].

2.1.3. FMO analysis

Frontier molecular orbital (FMO) analysis was carried out on the optimized geometries at the same level of theory (M06-2X/6-311+G(d,p)) in the gas phase. The HOMO and LUMO energies were extracted from the output files, and the HOMO–LUMO energy gap (E_g) was calculated as the difference between the LUMO and HOMO energies.

2.2. Experimental Details

2.2.1. Isolation and Chemical Characterization of AMEO

Aerial parts of *Abies marocana* were collected from Jbel Tazaout, Chefchaouen, Morocco, after obtaining the necessary permissions. We confirm that the collection of *Abies marocana* complied with all relevant institutional, national, and international guidelines and legislation and was carried out in accordance with the regulations set by the Tazaout and Talasemtane Forest authorities. Furthermore, the study was conducted in accordance with the IUCN Policy Statement on Research Involving Species at Risk of Extinction and the Convention on International Trade in Endangered Species of Wild Fauna and Flora (CITES). The plant specimen was identified and authenticated by Dr. Mohamed Kadiri, a botanist at the Laboratory of Applied Botany, Abdelmalek Essaâdi University, Morocco. A voucher specimen of *Abies marocana* was deposited in the herbarium of the Biology Department, Faculty of Sciences, Abdelmalek Essaâdi University, Morocco, under the code LAB-BIO-2025-067. The essential oil was obtained by steam distillation and stored at 4–6 °C until further use. GC/MS analysis was performed to identify the major constituents of the essential oil, with limonene as the predominant compound (38.46%), followed by *α*-pinene (21.96%), *β*-pinene (12.92%), and camphene (11.23%) (**Figure 1**). Limonene and pinene isomers are generally recognized as safe and are widely used in foods and household products, showing no evidence of acute or severe toxicity in humans under normal exposure conditions [44]. Similarly, available safety assessments indicate that camphene also exhibits low toxicity under typical exposure scenarios [45].

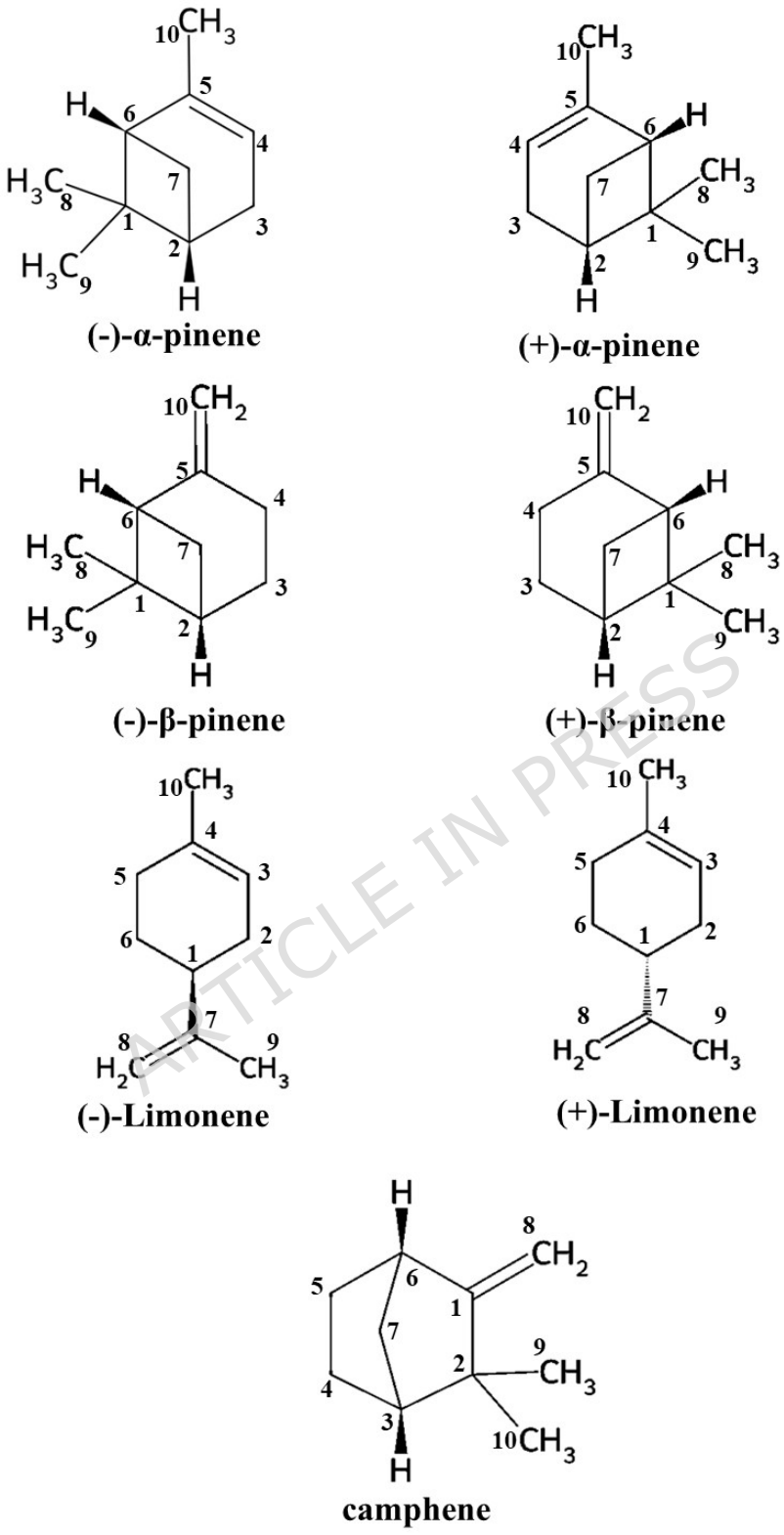

Figure 1. Two-dimensional chemical structures of AMEO compounds.

2.2.2. Preparation of Flexible Polyurethane Foam and AMEO as Additives (FPUF/AMEO)

FPUF samples were synthesized using a one-pot free foaming method. The polyol (Ongropur D6575, 40 g) was placed in a 1 L paper cup. The isocyanate (Ongronat XP1142, 20 g) was then added, both, from Wanhua-BorsodChem in Kazincbarcika, Hungary. AMEO was added at different weight percentages (0.00, 0.25, 0.50, 0.75, and 1.00%; **Table 1**) relative to the total PU formulation. The mixture was mixed for 8 s. The formulation and foaming processes were monitored using a FOAMAT 285 foam qualification system. The test duration was 300 s, during which the maximum exothermic temperature reached 25.9 °C. The foam was allowed to rise freely in the paper cup at room temperature. AMEO was incorporated as an additive into the FPUF, and the mechanical properties of the resulting samples were evaluated. Cylindrical specimens with a diameter of 30 mm and an approximate height of 30–33 mm were cut from each foam sample and used for the mechanical tests. All measurements were carried out in triplicate, both before and after dry ageing to evaluate the effect of long-term material use. The corresponding raw data from the triplicate measurements are provided in the Supplementary Information (**Tables S1 and S2**). The extent of the change was determined by the evaluation of the compression-force–deflection curves (decrease in force). If the degree of change was too large (higher than 15%), the material was considered unsuitable for further use under compressive stress [46].

The reduction in compression force was calculated according to **Equation 6**:

$$\Delta F_{50\%}(\%) = \frac{F_{50\%,0} - F_{50\%,1}}{F_{50\%,0}} \times 100 \qquad \textbf{Equation 6}$$

where $\Delta F_{50\%}$ – force measured at 50% compression, $F_{50\%,0}$ – force measured at 50% compression before dry heat ageing, and $F_{50\%,1}$ – force measured at 50% compression after dry heat ageing.

Similarly, the decrease in sample height was determined using **Equation 7**:

$$\Delta h = \frac{h_0 - h_1}{h_0} \qquad \textbf{Equation 7}$$

where Δh – decrease in height of the sample after dry heat ageing, h_0 – height of the original sample, h_1 – height of the sample after dry heat ageing.

Table 1. Formulation of flexible polyurethane foam and AMEO as additive (FPUF/AMEO)

Sample ID	Percentage of AMEO (% wt)	Weight of AMEO (g)	Polyol Premix Ongropur D6575 (g)	Isocyanate ongronat xp 1142 (g)
Reference	0.00	0.00	40	20
AMEO1	0.25	0.15	40	20
AMEO2	0.50	0.30	40	20

AMEO3	0.75	0.45	40	20
AMEO4	1.00	0.60	40	20

2.2.3. Dry heat ageing

A standard ageing test was performed to assess the impact of prolonged use of the foams. For the test, the ASTM D3574 Test K dry heat ageing procedure was followed. The samples were aged for 24 h at 140 ± 2°C in a laboratory drying oven (POL-EKO Aquaterra SLW240, Wodzislaw Slaski, Poland). Following the ageing process, a minimum of two hours of conditioning under the specified parameters (23 ± 2 °C and 50 ± 5% relative humidity) was performed, and the mechanical measurements were repeated, and the resulting changes compared to the pre-ageing were evaluated.

2.2.4. Mechanical Measurements

The mechanical properties of the prepared samples (reference and FPUF/AMEO) were evaluated using Test Method C of ASTM D3574, the standard test method for FPUFs [47]. Compression force deflection (CFD) was determined by compressing the samples over their entire surface to 50% of their original height, holding the compression for 1 min, and then measuring the force required to maintain the deformation.

2.2.5. FTIR Characterization

The functional groups of the unmodified FPUF and AMEO-containing FPUF samples were analyzed by Fourier transform infrared spectroscopy (FTIR) using a Bruker Vertex 70 spectrometer equipped with a Platinum ATR accessory (A225/Q, Multiple Crystals Diamond S1558DCCE). Spectra were recorded at room temperature over the wavenumber range of 400–4000 cm^{-1} with a resolution of 4 cm^{-1} and averaged over 32 scans in absorbance mode. Data acquisition was performed in double-sided, forward–backward mode using an RT-DLaTGS detector.

3. Experimental Results

3.1. Computational Results

3.1.1. Optimized Geometries

In this work, seven natural compounds from AMEO, (+)-*α*-pinene, (−)-*α*-pinene, (+)-*β*-pinene, (−)-*β*-pinene, (+)-limonene, (−)-limonene and camphene previously identified as major constituents in our earlier studies [48] were optimized in the gas, water, and ethylene glycol phases using the M06-2X functional (**Figure 2**). Because the (+) and (–) enantiomers showed identical C–H bond characteristics, the results are reported once per compound. Analysis of the C–H bond lengths revealed that the shortest bond was C10–H in *β*-pinene (1.084 Å), whereas the longest bond was C1–H in limonene (1.101 Å) (**Table 2**). Cartesian

coordinates of the optimized AMEO compounds calculated at the M06-2X/6-311+G(d,p) level of theory are provided in the Supplementary Information.

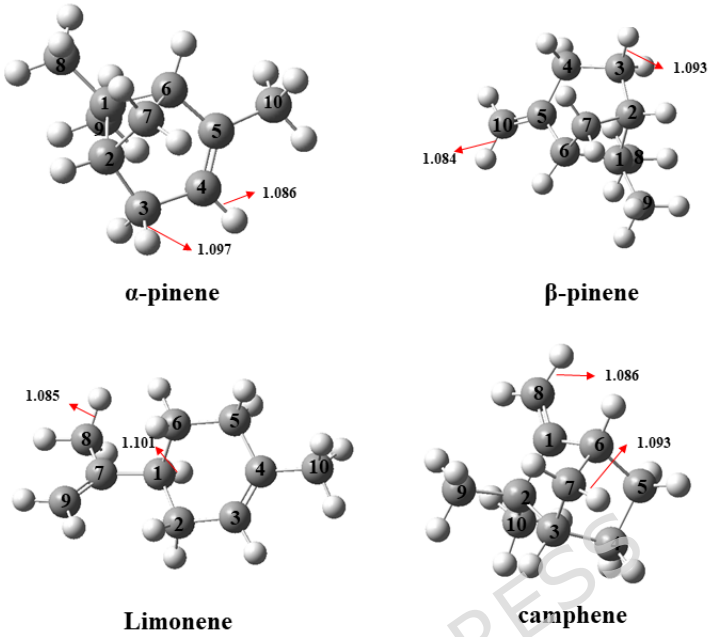

Figure 2. Three-dimensional structure of AMEO compounds optimized at the M06-2X/6-311+G(d,p) level of theory, and the appropriate bond lengths (in Å) for the strongest and weakest C–H bond

Table 2. Bond lengths (B.L.) (in Å) and bond dissociation enthalpy (BDE), ionization potential (IP), proton dissociation enthalpy (PDE), proton affinity (PA), and electron transfer enthalpy (ETE) values in kJ/mol of AMEO compounds computed using the M06-2X/6-311+G(d,p) level of theory in the gas phase

compounds	B.L.	BDE	IP	PDE	IP+PDE	PA	ETE	PA+ETE
Camphene			817.1					
C3-H	1.092	442.1		938.4	1755.5	1697.0	58.5	1755.5
C4-H	1.089	403.6		897.5	1714.5	1708.8	5.7	1714.5
C7-H	1.093	428.6		922.5	1739.6	1690.6	49.0	1739.6
C8-H	1.086	455.8		949.6	1766.7	1678.9	87.8	1766.7
C9-H	1.091	418.1		912.0	1729.1	1705.9	23.2	1729.1
***α*-pinene**			777.9					
C2-H	1.093	428.7		961.7	1739.7	1712.5	27.1	1739.7
C3-H	1.096	352.0		885.0	1663.0	1627.0	35.9	1663.0
C4-H	1.086	460.4		993.4	1771.3	1683.4	88.0	1771.3
C6-H	1.093	434.4		967.4	1745.4	1700.4	45.0	1745.4
C7-H	1.088	420.9		953.9	1731.8	1707.2	31.0	1738.2
C9-H	1.089	412.1		945.1	1723.0	1705.9	19.0	1724.9
C10-H	1.091	355.5		888.5	1666.4	1607.5	58.9	1666.4
***β*-pinene**			794.3					
C2-H	1.093	427.2		943.8	1738.1	1705.5	32.7	1738.1

C3-H	1.093	400.0		916.6	1710.9	1705.5	5.4	1710.9
C4-H	1.092	347.3		863.9	1658.2	1599.3	58.9	1658.2
C6-H	1.092	432.1		948.7	1743.0	1693.4	49.6	1743.0
C7-H	1.092	423.5		940.1	1734.4	1706.5	27.9	1734.4
C9-H	1.095	413.8		867.1	1661.4	1595.6	54.5	1650.1
C10-H	1.084	461.3		977.9	1772.2	1688.1	84.1	1772.2
Limonene			804.3					
C1-H	1.101	353.5		860.1	1664.4	1602.3	62.2	1664.4
C2-H	1.095	347.1		853.8	1658.1	1621.9	36.7	1658.6
C3-H	1.087	452.7		959.2	1763.4	1687.4	76.3	1763.7
C5-H	1.098	354.6		861.2	1665.5	1618.3	47.2	1665.5
C6-H	1.092	407.6		914.3	1718.6	1698.2	20.4	1718.6
C8-H	1.085	458.6		965.2	1769.5	1688.2	81.3	1769.5
C9-H	1.094	365.8		872.5	1676.7	1607.9	68.9	1676.7
C10-H	1.095	368.4		875.0	1679.3	1627.9	51.4	1679.3

3.1.2. Antioxidant Capability and Scavenging Mechanisms

The antioxidant efficacy of AMEO species was evaluated according to different mechanisms to assess their potential applicability as additives in polymer formulations.

Starting with the hydrogen atom transfer (HAT) mechanism, the most reactive bonds are those with the lowest BDE values [49], as hydrogen atoms can be donated from multiple positions within the antioxidant molecule. The HAT mechanism occurs through a single-step hydrogen atom transfer process, resulting in the formation of a radical [50]. The calculated BDE values of all AMEO compounds are listed in **Table 2**.

The bond dissociation enthalpy (BDE) values for all AMEO compounds were calculated in the gas phase using the M06-2X method. To assess the effect of the solvent on antioxidant activity, the most favorable C–H position (the lowest BDE) identified in the gas phase for each compound was further evaluated in water and ethylene glycol. The results showed that the same reactive sites remained the most favorable in both solvents, with only slight variations in BDE values (**Table 3)**.

Table 3. Comparison of the lowest BDE values (in kJ/mol) and most favorable C–H positions of AMEO compounds in gas phase, water, and ethylene glycol.

compounds	Best C–H position	BDE (gas)	BDE (water)	BDE (ethylene glycol)
Camphene	C4-H	403.6	404.3	404.1
α-pinene	C3-H	352.0	356.0	353.9
β-pinene	C4-H	347.3	353.1	350.9
Limonene	C2-H	347.1	352.2	349.8

This consistency suggests that the preferred hydrogen atom donation sites are not significantly influenced by the solvent environment, thereby confirming the reliability of the gas-phase predictions. The calculated C–H bond BDEs in the gas phase of AMEO compounds ranged from 347.1 to 461.3 kJ/mol (**Table 2**). The weakest bonds were found in limonene isomers. Among all evaluated sites, the C2–H position in limonene isomers displayed the lowest BDE in the gas phase (347.1 kJ/mol). Comparable values were obtained in water (352.2 kJ/mol) and ethylene glycol (349.8 kJ/mol) (**Table 3)**, suggesting that this site remains the most favorable for hydrogen atom donation regardless of the surrounding medium. These results indicate that limonene contains the most favorable sites for hydrogen atom donation. In contrast, the strongest bonds were observed in *β*-pinene isomers. The C10–H position exhibited the highest BDE value, 461.3 kJ/mol, in the gas phase.

Interestingly, additional weak sites were identified (C4**–**H) in *β*-pinene isomers, with BDE values of 347.3 kJ/mol in the gas phase. Only minor differences were observed in solution, with values of 353.1 kJ/mol in water and 350.9 kJ/mol in ethylene glycol, all of which are close to the lower limit of the overall range (347.1 kJ/mol). This suggests that both limonene and *β*-pinene possess favorable C–H sites for hydrogen atom donation, highlighting their potential as efficient free radical scavengers.

For *α*-pinene, analysis of the BDE values showed that the C3–H position is the weakest site, with a BDE of 352.0 kJ/mol in the gas phase. This suggests that this position is the most favorable for hydrogen atom donation compared to other C–H bonds within the same molecules. In the case of camphene, the weakest site was located at C4–H, with a BDE of 403.6 kJ/mol.

In the SET-PT mechanism, the first step is electron transfer from the antioxidant (A) to the radical, forming a radical cation ($A^{\bullet+}$), which then deprotonates to give a neutral radical (A•). To evaluate the antioxidant activity of the C–H site, the ionization potential (IP) and proton dissociation enthalpy (PDE) were calculated [20,32].

IPs and PDE values for AMEO compounds were computed in the gas phase **(Table 2).** The results indicate that the IP of *α*-pinene (777.9 kJ/mol) is the lowest, while camphene has the highest (817.1 kJ/mol). The PDE values of the C–H bonds vary significantly, ranging from 853.8 kJ/mol (C2–H in limonene) to 993.4 kJ/mol (C4–H in *α*-pinene) in the gas phase, indicating notable differences in the ease of proton loss depending on the molecular position. Notably, the same C–H positions identified as most reactive in the PDE analysis were also observed in the BDE results, indicating a consistent reactivity pattern across different antioxidant mechanisms. Consequently, the C2–H bond in limonene exhibits higher antioxidant

activity than the other C–H bonds, based on their IP + PDE values. The results obtained for the different C–H positions are consistent with the HAT results.

In the SPLET mechanism, the first step is proton loss from the antioxidant (A), forming an anionic species (A^-), which then donates an electron to the radical to give a neutral radical ($A^•$) [20]. To evaluate the antioxidant activity of the C–H site, the proton affinity (PA) and electron transfer enthalpy (ETE) were calculated. Lower PA and ETE values indicate a greater antioxidant ability of the studied molecule. The calculated PA and ETE for all the possible sites of C–H bonds of the AMEO compounds were collected and compared in the gas phase (**Table 2**). The PA values ranged from 1595.6 kJ/mol (*β*-pinene, C9–H) to 1712.5 kJ/mol (*α*-pinene, C2–H), and the ETE values ranged from 5.4 kJ/mol (*β*-pinene, C3–H) to 88.0 kJ/mol (*α*-pinene, C4–H). The most efficient SPLET site, based on the lowest PA+ETE sum, was *β*-pinene, C9–H (1650.1 kJ/mol). However, the PA+ETE value for limonene in C2–H was 1658.6 kJ/mol, which is very close, indicating that limonene is also highly favorable via SPLET. This aligns with limonene showing the most favorable antioxidant characteristics for the SET-PT and HAT mechanisms (**Table 2**).

Overall, based on the results, among the seven AMEO compounds, the C2–H bonds in limonene represent the most favorable antioxidant sites based on all three mechanisms (HAT, SET-PT, and SPLET). Several other C–H sites also show potential as effective free radical-scavengers. These theoretical results are in good agreement with our experimental data from a previous study on the antioxidant activity of AMEO, which showed weak radical scavenging activity in the DPPH assay but notable reducing power in the ferric reducing antioxidant power (FRAP) assay [48].

3.1.3. Frontier Molecular Orbital (FMO) Analysis

Frontier molecular orbital (FMO) analysis was employed to investigate the reactivity and electronic properties of the system. The energies of the highest occupied molecular orbital (HOMO) and lowest unoccupied molecular orbital (LUMO) are important quantum chemical descriptors that play a major role in the chemical reactivity of antioxidants [36]. The visual representations of the HOMO and LUMO electron density distributions, together with the energy gap (E_g) of the major compounds of AMEO are represented in **Figure 3**.

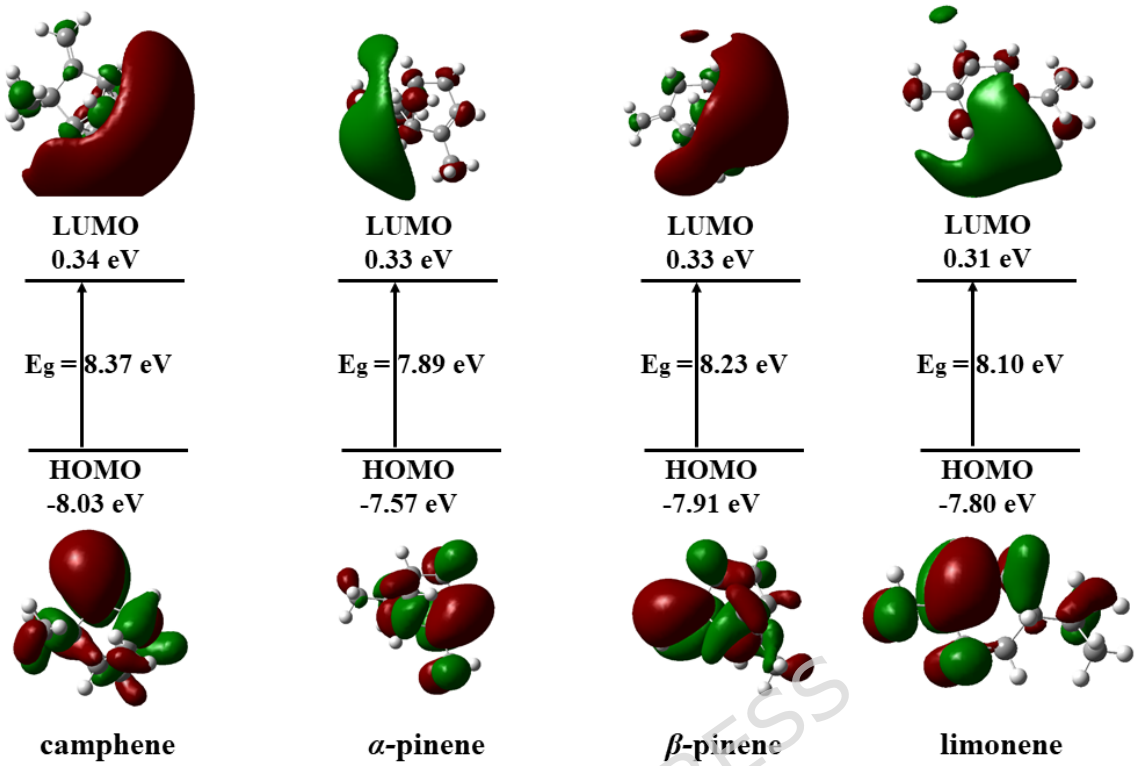

Figure 3. HOMO and LUMO orbital representations and energy gaps (E_g) of representative AMEO constituents calculated at the M06-2X/6-311+G(d,p) level of theory in the gas phase.

Among the studied compounds, *α*-pinene exhibited the highest HOMO energy (-7.57 eV), followed by limonene (-7.80 eV), *β*-pinene (-7.91 eV), and camphene (-8.03 eV), suggesting that α-pinene and limonene have the greatest intrinsic electron-donating tendencies.

The energy gap (E_g) is a measure of molecular chemical reactivity (a smaller energy gap indicates higher reactivity [34]). *α*-pinene exhibited the smallest E_g (7.89 eV) among all compounds, followed by limonene (8.10 eV), *β*-pinene (8.23 eV), and camphene (8.37 eV). The relatively small gap of *α*-pinene and limonene is consistent with their higher overall chemical reactivity and supports their superior radical-scavenging ability as identified by the BDE and SPLET calculations.

3.2. Experimental Results

3.2.1. Characterization of AMEO

The essential oil extracted from the aerial part of *Abies marocana* via steam distillation had a yield of 0.24%. GC/MS analysis of AMEO identified its major components, summarized in **Table 4**. Quantitative analysis revealed that limonene was the predominant compound (38.46%), followed by *α*-pinene (21.96%), *β*-pinene (12.92%), and camphene (11.23%) [48].

Table 4. Major chemical components (relative area percentage) of AMEO by determined by GC/MS.

N°	*Compounds*	*MF*	*MW (g/mol)*	*RI*	*RT (min)*	*Area (%)*
1	*α*-Pinene	$C_{10}H_{16}$	136	929	8.83	21.16
2	Camphene	$C_{10}H_{16}$	136	952	9.14	11.23
3	*β*-Pinene	$C_{10}H_{16}$	136	987	9.95	12.92
4	Limonene	$C_{10}H_{16}$	136	1004	11.73	38.46

MF: Molecular Formula; MW: Molecular Weight; RI: Retention Index; RT: Retention time

3.2.2. Mechanical Tests

The addition of antioxidant additives to flexible polyurethane foam can significantly influence its mechanical properties, particularly the compression force (F). The BDE of antioxidants plays a key role in determining the stability of polyurethane materials. Compound with higher oxidative stability can help maintain the mechanical properties of polyurethane foams over longer periods by reducing degradation. Therefore, selecting antioxidants with suitable BDE values is essential to minimize oxidative damage and preserve the foam's mechanical integrity, particularly its resistance to compression [20].

Compression force deflection (CFD) tests were carried out in accordance with ASTM D3574 Test C on FPUF samples prepared with AMEO as an additive at concentrations of 0.00 (Ref), 0.25, 0.50, 0.75, and 1.00 wt%. The samples were further subjected to dry heat ageing following ASTM D3574 Test K. The final force values ($F_{50\%,0}$; $F_{50\%,1}$) were recorded at 50% compression of the original sample height after one minute. Following ageing, the changes in compression force and sample height were determined (**Table 5**).

It is evident from the results that the $\Delta F_{50\%}$% after ageing is considerably higher in all samples than the 15% limit set by the standard, indicating that mechanical deterioration occurs upon long-term ageing regardless of the formulation. The reference sample showed a compression-force loss of 25.46%, while the AMEO-modified samples exhibited values of 22.70% (0.25 wt%), 23.65% (0.50 wt%), 24.71% (0.75 wt%), and 21.88% (1.0 wt%).

Although the calculated $\Delta F_{so\%}$ values did not show a strictly monotonic dependence on AMEO concentration, this parameter is derived from the force values measured before and after ageing. As shown in **Figure S1** (Supplementary Information), the individual compression force values before ($F_{so\%,0}$) and after ($F_{so\%,1}$) dry heat ageing exhibited a generally consistent trend with increasing AMEO content. The apparent variation in $\Delta F_{so\%}$ therefore results from the normalization of the force loss by the initial compression force value, where small changes in either parameter can affect the calculated percentage. Although none of the formulations fully meet the ASTM threshold, the AMEO-modified samples consistently exhibited lower

compression-force loss than the unmodified reference. Compared with the reference, the reductions ranged from 0.75 to 3.58 percentage points, corresponding to approximately 2.95–14.06% relative improvement in compression-force retention. This suggests that AMEO may contribute to improved retention of the mechanical properties of polyurethane foam during thermal ageing, slowing the deterioration process even if it does not completely prevent it. However, the detailed interactions with oxygen-centered radicals such as peroxy ($ROO^{\bullet}$) and alkoxy ($RO^{\bullet}$) radicals, which are central to polyurethane degradation mechanisms, were not specifically investigated in the present study. Among the formulations tested, the 1.0 wt% AMEO formulation showed the lowest compression-force loss, indicating improved retention of compression force after ageing under the conditions investigated. These findings indicate that AMEO has potential as a bio-based additive for enhancing the ageing performance of polyurethane foam. However, additional oxidation-sensitive analyses are required to confirm the proposed stabilization mechanism. Furthermore, although polyurethane foams containing AMEO may have potential for future food-packaging applications, their suitability cannot be established based on the present study. Further investigations, including migration, toxicity, additive retention, and application-specific performance tests, are required before such applications can be considered.

Table 5. Compression test results (ASTM D3574 Test C) before and after dry-heat ageing for FPUF samples prepared with AMEO as an additive at concentrations of 0.00 (Ref), 0.25, 0.50, 0.75, and 1.00 wt%.

Sample ID	$F_{50\%,0}$ (N) ± SD	$F_{50\%,1}$ (N) ± SD	$\Delta F_{50\%}$ (%) ± SD	h_0 (mm) ± SD	h_1 (mm) ± SD	Δh (%) ± SD
Reference	5.46 ± 0.81	4.07 ± 0.62	25.46 ± 1.36	29.53 ± 0.64	29.84 ± 0.63	-1.05 ± 0.11
AMEO1	5.55 ± 0.76	4.29 ± 0.60	22.70 ± 1.76	30.33 ± 0.63	30.5 ± 0.68	-0.56 ± 0.15
AMEO2	5.75 ± 1.13	4.39 ± 0.77	23.65 ± 2.02	29.58 ± 0.30	29.52 ± 0.33	0.20 ± 0.08
AMEO3	6.11 ± 0.48	4.60 ± 0.39	24.70 ± 0.69	29.75 ± 0.40	29.32 ± 0.39	1.45 ± 0.12
AMEO4	6.26 ± 1.28	4.89 ± 0.84	21.88 ± 1.28	29.78 ± 0.96	29.52 ± 0.96	0.87 ± 0.04

Values are presented as mean ± SD (n = 3).

Compression force–deflection curves for the reference (Ref) and AMEO-modified FPUF samples before and after dry heat ageing, measured up to 50% of the original sample height **(Figure 5).** The curves also include the one-minute hold at the compressed height, during which a decrease in force is observed due to relaxation of the elastic foam. The AMEO-modified samples retain slightly higher compression forces than the aged reference, indicating a modest stabilizing effect of the additive across the concentrations tested (0.15, 0.30, 0.45, and 0.60 g).

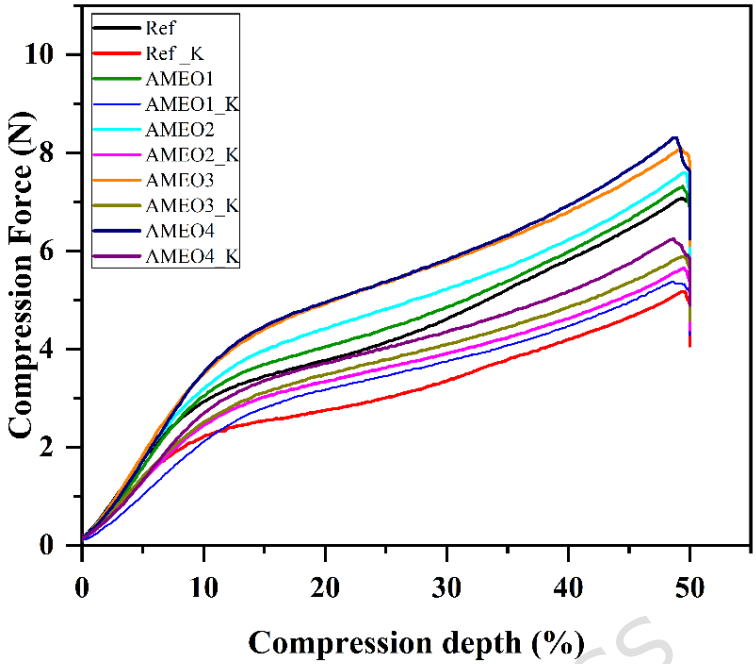

Figure 4. ASTM D3574 Test C (Compression Force Deflection) measured at 50% sample height before and after dry-heat ageing (ASTM D3574 Test K) for FPUF samples prepared with AMEO as an additive at concentrations of 0.00 (Ref), 0.25, 0.50, 0.75 and 1.00 wt %. The curves shown are representative measurements.

3.2.3. FTIR Analysis

To further investigate the nature of the interaction between the studied essential oil and the FPUF, FTIR analysis was performed on the reference FPUF and FPUF/AMEO samples with different AMEO loadings (AMEO1-AMEO4) **(Figure S2**, Supplementary Information). The FTIR spectra exhibited the same characteristic polyurethane bands before and after the incorporation of AMEO, including N–H group stretching vibration observed at 3300 cm^{-1}. The asymmetric and symmetric stretching vibrations of C–H groups (–CH_2– and –CH_3) appeared at 2967 and 2875 cm^{-1}, respectively. The band observed in the range of 1680–1740 cm^{-1} corresponds to the stretching vibration of carbonyl (C=O) group present in the structure of urethane bonds. The N–H bending vibration was found at 1596 cm^{-1}, while the characteristic peak connected with stretching vibration of C–N bond appears at 1526 cm^{-1}. The ether bond (C–O–C) stretching vibration was observed at 1140 cm^{-1}. In addition, the peaks at wavenumbers ranging from 1360–1477 cm^{-1} are characteristic of the bending vibrations of methyl and methylene groups originating from the polyol chains [51]. No new absorption bands or significant shifts in peak positions were observed after AMEO incorporation. This result is consistent with the chemical nature of the major AMEO constituents, including limonene, *α*-pinene, *β*-pinene, and camphene, which together represent 83.77% of the total compounds and are mainly hydrocarbons lacking functional groups capable of reacting with isocyanate groups (–NCO).

The absence of new covalent bonds confirms that the studied oil acts as a physical antioxidant additive within the polyurethane network rather than through chemical integration into the polymer backbone.

4. Conclusion

In conclusion, compounds identified in *Abies marocana* essential oil were assessed through DFT calculations to evaluate their antioxidant potential via three mechanistic pathways: HAT, SET-PT, and SPLET, characterized by the thermodynamic descriptors BDE, IP, PDE, PA, and ETE, in both gas and solvent phases. Limonene was found to be the predominant compound (38.46%), followed by α-pinene (21.96%), β-pinene (12.92%), and camphene (11.23%). Among all studied constituents, limonene isomers exhibited the most favorable thermodynamic parameters across all three mechanisms, confirming their higher radical-scavenging ability. FMO analysis further supported these findings, with α-pinene exhibiting the smallest HOMO–LUMO energy gap, followed by limonene, supporting their higher chemical reactivity and radical-scavenging potential among the studied AMEO constituents. Based on its abundance and calculated thermodynamic descriptors, limonene may contribute to the observed response, although its individual effect was not experimentally isolated. AMEO was incorporated into flexible polyurethane foam at different concentrations. Compression tests before and after dry heat ageing revealed that AMEO-modified foams showed slightly better compression-force retention than the reference sample. The absolute compression force values increased with AMEO loading, while the calculated percentage force loss was generally lower for AMEO-modified samples, indicating improved ageing resistance. FTIR characterization of the FPUF and FPUF/AMEO samples revealed similar spectra profiles with no new peaks, confirming that AMEO components did not react with the isocyanate groups during foam synthesis. This is consistent with the purely hydrocarbon nature of the major terpene constituents. The stabilization mechanism is therefore physical in nature, consistent with the antioxidant mechanisms identified by DFT calculations. These results suggest that AMEO can act as a multifunctional additive, providing both antioxidant activity and mechanical tuning in polyurethane foams. Future studies, including migration testing, toxicological evaluation, and real-world application testing will be necessary to further assess the potential of AMEO-modified polyurethane foams for specific end-use applications.

Acknowledgement

Additional support was provided by the University Research Scholarship Program of the Ministry for Culture and Innovation, funded by the National Research, Development and Innovation Fund This research was supported by the Centre National de la Recherche Scientifique et Technique (CNRST) through the PhD-Associate Scholarship – PASS program in Morocco. BF thanks the support by the János Bolyai Research Scholarship of the Hungarian Academy of Sciences. We acknowledge the Digital Government

Development and Project Management Ltd. for awarding us access to the Komondor HPC facility based in Hungary. Calculations have also been carried out using resources provided by Wroclaw Centre for Networking and Supercomputing (http://wcss.pl).

Funding

This work was funded by the Centre National de la Recherche Scientifique et Technique (CNRST) under the PhD-Associate Scholarship – PASS program (Morocco). Furthermore, DM and RB thanks the University Research Scholarship Program of the Ministry for Culture and Innovation (Hungary), supported by the National Research, Development and Innovation Fund. BF thanks the support by the János Bolyai Research Scholarship of the Hungarian Academy of Sciences.

Data Availability Statement

Data will be made available on request.

REFERENCES

1 Fierascu, R. C., Fierascu, I., Baroi, A. M. & Ortan, A. Selected Aspects Related to Medicinal and Aromatic Plants as Alternative Sources of Bioactive Compounds. *Int. J. Mol. Sci.* **22**, 1521, doi:10.3390/ijms22041521 (2021).

2 Boukhatem, M. N. & Setzer, W. N. Aromatic herbs, medicinal plant-derived essential oils, and phytochemical extracts as potential therapies for coronaviruses: future perspectives. *Plants* **9**, 800, doi:10.3390/plants9060800 (2020).

3 Sharma, S., Barkauskaite, S., Jaiswal, A. K. & Jaiswal, S. Essential oils as additives in active food packaging. *Food Chem.* **343**, 128403, doi:10.1016/j.foodchem.2020.128403 (2021).

4 El Sawi, S. A., Ibrahim, M. E., El-Rokiek, K. G. & El-Din, S. A. S. Allelopathic potential of essential oils isolated from peels of three citrus species. *Ann. Agric. Sci.* **64**, 89-94, doi:10.1016/j.aoas.2019.04.003 (2019).

5 Kant, R. & Kumar, A. Review on essential oil extraction from aromatic and medicinal plants: Techniques, performance and economic analysis. *Sustain. Chem. Pharm* **30**, 100829, doi:10.1016/j.scp.2022.100829 (2022).

6 Zarith Asyikin Abdul, A. *et al.* Essential Oils: Extraction Techniques, Pharmaceutical And Therapeutic Potential - A Review. *Curr. Drug Metab.* **19**, 1100-1110, doi:10.2174/1389200219666180723144850 (2018).

7 Zhang, L. & Piao, X. Use of aromatic plant-derived essential oils in meat and derived products: Phytochemical compositions, functional properties, and encapsulation. *Food Biosci.* **53**, 102520, doi:10.1016/j.fbio.2023.102520 (2023).

8 Teshome, E., Forsido, S. F., Rupasinghe, H. P. V. & Olika Keyata, E. Potentials of Natural Preservatives to Enhance Food Safety and Shelf Life: A Review. *Sci. World J.* **2022**, 9901018, doi:10.1155/2022/9901018 (2022).

9 Sendón, R. *et al.* Detection of migration of phthalates from agglomerated cork stoppers using HPLC-MS/MS. *J. Sep. Sci.* **35**, 1319-1326, doi:10.1002/jssc.201100871 (2012).

10 Bhavaniramya, S., Vishnupriya, S., Al-Aboody, M. S., Vijayakumar, R. & Baskaran, D. Role of essential oils in food safety: Antimicrobial and antioxidant applications. *Grain Oil Sci. Technol.* **2**, 49-55, doi:10.1016/j.gaost.2019.03.001 (2019).

11 Ribeiro-Santos, R., Andrade, M., Melo, N. R. d. & Sanches-Silva, A. Use of essential oils in active food packaging: Recent advances and future trends. *Trends Food Sci. Technol.* **61**, 132-140, doi:10.1016/j.tifs.2016.11.021 (2017).
12 Wen, P. *et al.* Encapsulation of cinnamon essential oil in electrospun nanofibrous film for active food packaging. *Food Control* **59**, 366-376, doi:10.1016/j.foodcont.2015.06.005 (2016).
13 Marcos, B. *et al.* Development of biodegradable films with antioxidant properties based on polyesters containing α-tocopherol and olive leaf extract for food packaging applications. *Food Packag. Shelf Life* **1**, 140-150, doi:10.1016/j.fpsl.2014.04.002 (2014).
14 Al-Malaika, S., Issenhuth, S. & Burdick, D. The antioxidant role of vitamin E in polymers V. Separation of stereoisomers and characterisation of other oxidation products of dl-α-tocopherol formed in polyolefins during melt processing. *Polym. Degrad. Stabil.* **73**, 491-503, doi:10.1016/S0141-3910(01)00137-9 (2001).
15 Stoleru, E. & Brebu, M. Stabilization techniques of essential oils by incorporation into biodegradable polymeric materials for food packaging. *Molecules* **26**, 6307, doi:10.3390/molecules26206307 (2021).
16 Moukrim, S. *et al.* Climate change impact on potential distribution of an endemic species Abies marocana Trabut. *Ekológia* **41**, 329-339, doi:10.2478/eko-2022-0034 (2022).
17 Khemani, K. C. Polymeric foams: an overview. *ACS Symp. Ser*, doi:10.1021/bk-1997-0669.ch001 (1997).
18 Titow, M. *PVC technology*. (Springer Science & Business Media, 2012).
19 Eaves, D. *Handbook of polymer foams*. (iSmithers Rapra Publishing, 2004).
20 Thbayh, D. K. *et al.* α-Tocopherol and Trolox as Effective Natural Additives for Polyurethane Foams: A DFT and Experimental Study. *Molecules* **29**, 6037, doi:10.3390/molecules29246037 (2024).
21 Zhang, J., Yeoh, G. H. & Kabir, I. I. Polyurethane Materials for Fire Retardancy: Synthesis, Structure, Properties, and Applications. *Fire* **8**, 64, doi:10.3390/fire8020064 (2025).
22 Suleman, S., Khan, S. M., Jameel, T., Aleem, W. & Shafiq, M. Synthesis and characterization of flexible and rigid polyurethane foam. *Asian J. Appl. Sci.* **2** (2014).
23 Suleman, S. *et al.* A comprehensive short review on polyurethane foam. *Int. J. Innov. Sci. Res* **12**, 165-169 (2014).
24 Fan, X., Wang, H., Kong, L. & Huang, J. Advanced ethylene-absorbing and cushioning depending on the 3D porous-structured fruit packaging: Toward polyurethane foam manipulation using zein and soybean oil polyol substrates. *Food Res. Int* **186**, 114340, doi:10.1016/j.foodres.2024.114340 (2024).
25 Idah, P., Ajisegiri, E. & Yisa, M. Fruits and vegetables handling and transportation in Nigeria. *AU Journal of Technolog* (2007).
26 Ruiz-Altisent, M. Damage mechanisms in the handling of fruits. In: "Progress in agricultural physics and engineering". C.A.B. International, Walingford (UK), pp. 231-257. (1991).
27 Gao, Y. Research on properties and design methods of cushion packaging materials for consumer electronics. (2018).
28 Ates, M., Karadag, S., Eker, A. A. & Eker, B. Polyurethane foam materials and their industrial applications. *Polym. Int* **71**, 1157-1163, doi:10.1002/pi.6441 (2022).
29 Yuan, Y., Guo, Q., Xu, L. & Wang, W. Rigid Polyurethane Foam Derived from Renewable Sources: Research Progress, Property Enhancement, and Future Prospects. *Molecules* **30** (2025).
30 Zhang, S. *et al.* High-performance flexible polyurethane from renewable castor oil: Preparation, properties and mechanism. *Composites Part A: Applied Science and Manufacturing* **159**, 107034 (2022).
31 Rohman, R., Nath, R. & Kar, R. Revisiting the hydrogen atom transfer reactions through a simple and accurate theoretical model: Role of hydrogen bond energy in polyphenolic antioxidants. *Comput. Theor. Chem.* **1223**, 114097, doi:10.1016/j.comptc.2023.114097 (2023).

32 Boulebd, H. Comparative study of the radical scavenging behavior of ascorbic acid, BHT, BHA and Trolox: Experimental and theoretical study. *Journal of Molecular Structure* **1201**, 127210, doi:10.1016/j.molstruc.2019.127210 (2020).

33 Álvarez-Diduk, R., Galano, A., Tan, D. X. & Reiter, R. J. The key role of the sequential proton loss electron transfer mechanism on the free radical scavenging activity of some melatonin-related compounds. *Theoretical Chemistry Accounts* **135**, 38, doi:10.1007/s00214-015-1785-5 (2016).

34 Chen, D. & Wang, H. HOMO-LUMO energy splitting in polycyclic aromatic hydrocarbons and their derivatives. *Proceedings of the Combustion Institute* **37**, 953-959, doi:10.1016/j.proci.2018.06.120 (2019).

35 Waleed, H. Q. *et al.* Crystallisation of 1,2-dimethylimidazole, and 1-methylimidazole with organic acids. *Sci. Rep.* **16**, 4127, doi:10.1038/s41598-025-34293-9 (2026).

36 Mahmoudi, S., Dehkordi, M. M. & Asgarshamsi, M. H. Density functional theory studies of the antioxidants—a review. *J. Mol. Model.* **27**, 271, doi:10.1007/s00894-021-04891-1 (2021).

37 Atkins, P. W., De Paula, J. & Keeler, J. *Atkins' physical chemistry*. (Oxford university press, 2023).

38 Frisch, M. *et al.* Gaussian 16 (Gaussian, Inc., Wallingford, CT, 2016). *J. Comput. Chem* **200**, 300-400 (2024).

39 Nikšić-Franjić, I. & Ljubić, I. Comparing the performances of various density functionals for modelling the mechanisms and kinetics of bimolecular free radical reactions in aqueous solution. *Phys. Chem. Chem. Phys.* **21**, 23425-23440, doi:10.1039/C9CP04688G (2019).

40 La Rocca, M. V. *et al.* Benchmarking the DFT methodology for assessing antioxidant-related properties: quercetin and edaravone as case studies. *J. Mol. Model.* **22**, 250, doi:10.1007/s00894-016-3118-6 (2016).

41 Thbayh, D. K., Reizer, E., Kahaly, M. U., Viskolcz, B. & Fiser, B. Antioxidant Potential of Santowhite as Synthetic and Ascorbic Acid as Natural Polymer Additives. *Polymers* **14**, 3518 (2022).

42 Thbayh, D. K. & Fiser, B. Computational study of synthetic and natural polymer additives — Antioxidant potential of BHA, TBHQ, BHT, and curcumin. *Polym. Degrad. Stab.* **201**, 109979, doi:10.1016/j.polymdegradstab.2022.109979 (2022).

43 Fifen, J. J. Thermodynamics of the Electron Revisited and Generalized. *J Chem Theory Comput* **9**, 3165-3169, doi:10.1021/ct400212t (2013).

44 Jin, K.-S. *et al.* Promises and Risks of Unsaturated Volatile Organic Compounds: Limonene, Pinene, and Isoprene: Limonene, Pinene, and Isoprene. *Food Sci. Biotechnol* **17**, 447-456 (2008).

45 Api, A. M. *et al.* RIFM fragrance ingredient safety assessment, camphene, CAS Registry Number 79-92-5. *Food Chem. Toxicol* **182**, 114212, doi:10.1016/j.fct.2023.114212 (2023).

46 Hornyák-Mester, E. *et al.* Comparative analysis of thermal degradation effects on traditional and low-emission flexible polyurethane foams. *Express Polym. Lett.* **18**, doi:10.3144/expresspolymlett.2024.74 (2024).

47 Tsioptsias, C., Gkouzouma, G., Leontiadis, K. & Tsivintzelis, I. Effect of an Antioxidant and a Compatibilizer on the Mechanical Properties of Virgin and Thermally Aged Polypropylene Drawn Fibers. *Textiles* **2**, 499-510, doi:10.3390/textiles2030028 (2022).

48 El Bakkali, M. *et al.* Composition and antioxidant activity of Abies marocana essential oil. *Scientific Reports*, doi:10.1038/s41598-026-38235-x (2026).

49 Boulebd, H. Comparative study of the radical scavenging behavior of ascorbic acid, BHT, BHA and Trolox: Experimental and theoretical study. *J. Mol. Struct.* **1201**, 127210, doi:10.1016/j.molstruc.2019.127210 (2020).

50 Trouillas, P., Marsal, P., Siri, D., Lazzaroni, R. & Duroux, J.-L. A DFT study of the reactivity of OH groups in quercetin and taxifolin antioxidants: The specificity of the 3-OH site. *Food Chem.* **97**, 679-688, doi:10.1016/j.foodchem.2005.05.042 (2006).

51 Alavi Nikje, M. M. & Nikrah, M. Glycerin as a new glycolysing agent for chemical recycling of cold cure polyurethane foam wastes in “split-phase” condition. *Polymer Bulletin* **58**, 411-423, doi:10.1007/s00289-006-0683-3 (2007).